

Exciton radiative lifetime in ZnO nanorods fabricated by vapor phase transport method

X. H. Zhang,^{a)} S. J. Chua, and A. M. Yong

Institute of Materials Research and Engineering, 3 Research Link, Singapore 117602, Singapore

H. Y. Yang, S. P. Lau, S. F. Yu, and X. W. Sun

School of Electrical and Electronic Engineering, Nanyang Technological University, Nanyang Avenue, Singapore 639798, Singapore

Lei Miao, Masaki Tanemura, and Sakae Tanemura

Department of Environmental Technology, Graduate School of Engineering, Nagoya Institute of Technology, Gokiso-cho, Showa-ku, Nagoya 466-8555, Japan

(Received 6 October 2006; accepted 2 December 2006; published online 3 January 2007)

The exciton radiative lifetime in ZnO nanorods is studied. It is found that the exciton radiative lifetime increases with temperature as T^2 . Furthermore, the spectral linewidth of the photoluminescence of the ZnO nanorods also increases with temperature as T^2 , suggesting a linear dependence of exciton radiative lifetime on the spectral linewidth. The physics behind is that the oscillator strength of excitons at $k=0$ is shared equally among all the states within the spectral linewidth and the coherence extension of an exciton decreases with temperature due to the scattering by phonons, defects, or impurities. © 2007 American Institute of Physics.

[DOI: 10.1063/1.2429019]

ZnO has attracted much attention recently because of its potential applications in optoelectronic devices operating in the ultraviolet to blue spectral region, owing to its direct wide band gap of 3.37 eV at room temperature.¹ Compared to other wide band gap semiconductors, ZnO has an extremely large exciton binding energy of 60 meV,^{2,3} which is much larger than the thermal energy at room temperature and therefore allows the survival of excitons at room temperature and above.⁴ Excitons therefore play important roles in the optical properties of ZnO. On the other hand, a wide variety of ZnO nanostructures have been fabricated.⁵ Excitons in geometrically confined systems exhibit different properties as compared to three-dimensional excitons as a result of the confinement.⁶⁻¹¹ For example, Guo *et al.*¹¹ experimentally found that the third order nonlinear susceptibility of ZnO nanoparticles is ~ 500 times larger than that of bulk ZnO. Theoretically, it has been shown that the exciton-photon coupling in ZnO quantum dots (QDs) is particularly strong and the exciton radiative recombination rate drastically varies with the dot size.^{12,13} Fonoberov and Balandin^{14,15} calculated the radiative lifetime of excitons in ZnO nanocrystals and predicted the size dependence of the exciton radiative lifetime. Zhang *et al.*¹⁶ have shown experimentally that the confinement of ZnO QDs can reduce the exciton radiative lifetime significantly. In this letter, we investigate the optical properties, especially the exciton radiative lifetime of ZnO nanorods. We find that the exciton radiative lifetime in ZnO nanorods increases with temperature and has a linear dependence on the spectral linewidth of the photoluminescence. The mechanism for the phenomena is discussed.

The ZnO nanorods used in present study were fabricated using the following procedure. Firstly, a SiO_x layer with thickness of 200 nm was formed on (001) silicon wafer by thermal annealing at 1000 °C. Then a 300-nm-thick ZnO

polycrystalline film was deposited onto the SiO_x layer using a filtered cathodic vacuum arc technique.¹⁶ Finally, ZnO nanorods were fabricated in a quartz tube using vapor phase transport method. The sample was first characterized using scanning electron microscope (SEM) and transmission electron microscope (TEM). The optical properties of the ZnO nanorods were characterized using time-integrated photoluminescence (TIPL), and time-resolved photoluminescence. The experimental setup has been described elsewhere.¹⁶

Figure 1 presents the SEM and TEM images of the ZnO nanorods. From the SEM image [Fig. 1(a)], it is seen that the nanorods grew almost vertically from the substrate. The diameter of the nanorods is about 100 nm and the length is about 2 μm . Figure 1(b) is the high resolution TEM image of a single ZnO nanorod, which clearly reveals a well resolved lattice of the ZnO nanorod. The electron diffraction pattern [the inset of Fig. 1(b)] exhibits bright electron diffraction spots corresponding to the crystal planes of the wurtzite structure, indicating that the ZnO nanorod has a single crystal hexagonal structure with good crystalline quality.

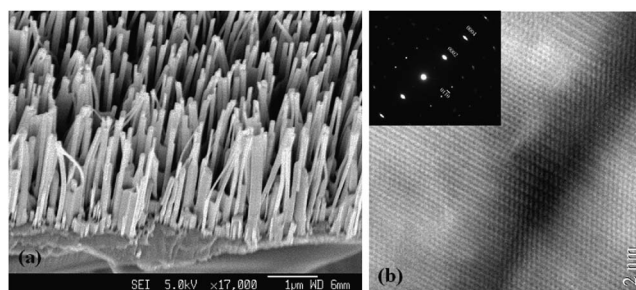


FIG. 1. SEM and TEM images of the ZnO nanorods fabricated. The SEM image (a) clearly shows the vertically aligned ZnO nanorods. The high resolution TEM image (b) of a single ZnO nanorod and the electron diffraction pattern (inset) show that the ZnO nanorod has a single crystal hexagonal structure with good crystalline quality.

^{a)}Electronic mail: xh-zhang@imre.a-star.edu.sg

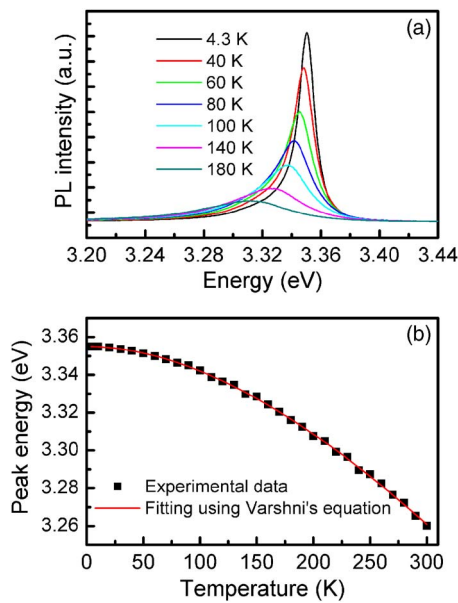


FIG. 2. (Color online) TIPL spectra of the ZnO nanorods measured at various temperatures (a) and the temperature dependence of the PL peak energy (b). The solid squares stand for experimental data while the solid curve is the least-squares fit using Varshni's equation.

Figure 2(a) plots the near-band-edge TIPL spectra of the ZnO nanorods measured at various temperatures. An emission band at 3.355 eV with a full width at half maximum (FWHM) of 13.6 meV was observed at 4.3 K. The ZnO layer deposited was polycrystalline and showed very weak luminescence before the fabrication of ZnO nanorods. However, the luminescence was significantly enhanced after the deposition of the ZnO nanorods. We therefore believe that the PL was mainly from the ZnO nanorods. Figure 2(b) plots the PL peak energy as a function of temperature from 4.3 to 300 K. The temperature dependence of the band gap energy of a semiconductor can be described by Varshni's equation,¹⁷

$$E_g(T) = E_g(0) - \alpha T^2 / (T + \beta), \quad (1)$$

where E_g is the band gap energy, and α and β are constants. In fact, it has been found that the temperature dependence of free exciton (FX) transition energy in ZnO can also be described by this equation.¹⁸ The least-squares fitting of the experimental data using Eq. (1) generates the fitting parameters $\alpha = 1.07 \times 10^{-3}$ eV/K and $\beta = 727$ K, which are in good agreement with the results by Wang and Giles.¹⁸ Fonoberov *et al.*¹⁹ conducted detailed PL studies of ZnO quantum dots, ZnO nanocrystals, and bulk ZnO crystal. They found that the near-band-edge PL of bulk ZnO crystal is dominated by bound exciton transitions at low temperature and FX related transitions take over the PL intensity at high temperature. For ZnO nanocrystals, they found that the near-band-edge PL evolves from the recombination of the acceptor-bound excitons at low temperature to the recombination of the donor-bound excitons at high temperature. However, the PL spectra we measured at various temperatures did not show such evolution. Furthermore, the temperature dependence of PL peak energy can be well described by Varshni's equation. Considering the fact that our measurements were done with the excitation of high intensity femtosecond pulses ($40 \mu\text{J}/\text{cm}^2$ per pulse), we believe that the measured PL spectra were dominated by FX recombinations. However, the PL peak en-

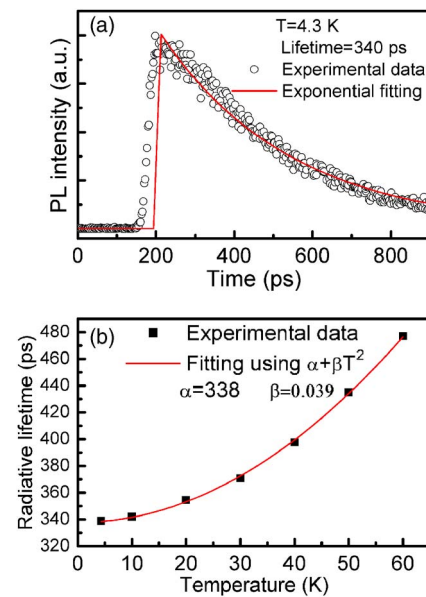


FIG. 3. (Color online) (a) Time evolution of the spectrally integrated PL of the ZnO nanorods measured at 4.3 K. (b) Exciton radiative lifetime as a function of temperature from 4.3 to 60 K. The solid squares stand for experimental data while the solid curve is the least-squares fit using $\alpha + \beta T^2$.

ergy of 3.355 eV at 4.3 K is 22 meV smaller than the reported FX transition energy of 3.377 eV at low temperature.²⁰ The difference might be explained with band gap renormalization due to the strong excitation.

Figure 3(a) presents the time evolution of the spectrally integrated PL intensity of the ZnO nanorods measured at 4.3 K. The PL decay trace can be well fitted using a single exponential function and a lifetime of 340 ps was obtained from the least-squares fitting. We now discuss whether the lifetime measured is the exciton radiative lifetime. It is well known that the photogenerated carriers can recombine through both radiative and nonradiative channels. If the recombination is dominated by nonradiative channels, the time and spectrally integrated PL intensity will show nonlinear increase with the excitation intensity.²¹ However, our measurement (not shown here) reveals a linear dependence of the time and spectrally integrated PL intensity on the excitation intensity, which evidences that the exciton radiative recombination is the dominating channel for the carrier recombination process. The further evidence comes from the temperature dependent exciton lifetimes, which is shown in Fig. 3(b). If the recombination process was dominated by nonradiative channels, the lifetime would decrease with increasing temperature, since the nonradiative channels would play a more important role with temperature. However, within the experimental uncertainties, the measured lifetime increases with temperature until 60 K. We therefore conclude that the exciton radiative recombination dominates the recombination process and the measured lifetimes are exciton radiative lifetimes below 60 K.

As shown in Fig. 3(b), the exciton radiative lifetime increases with temperature as T^2 . The temperature dependence of exciton radiative lifetime has been studied in other material systems. Feldmann *et al.*⁸ have shown that the exciton radiative lifetime in GaAs quantum wells is proportional to T when the spectral linewidth is much smaller than the thermal energy kT . Akiyama *et al.*²² demonstrated that the exciton radiative lifetime in GaAs quantum wires increases with

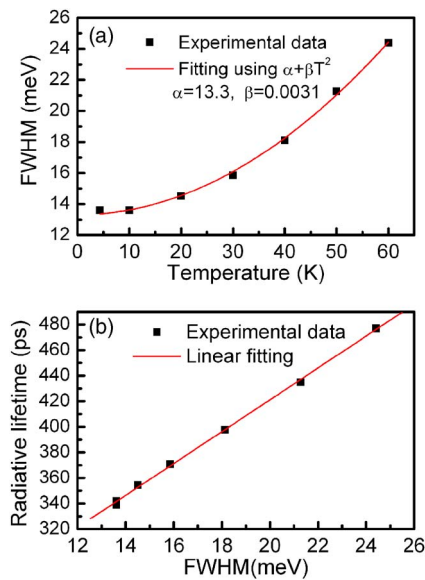


FIG. 4. (Color online) (a) FWHM of the PL spectra as function of temperature from 4.3 to 60 K. The solid squares stand for experimental data while the solid curve is the least-squares fit using $\alpha + \beta T^2$. (b) Spectral linewidth dependence of the exciton radiative lifetime. The solid squares stand for experimental data. The linear fit (solid line) is also plotted in the figure.

temperature as \sqrt{T} . It was also found that the exciton radiative lifetime in bulk GaAs increases with temperature.²³ The temperature dependence of exciton radiative lifetime can be understood in terms of thermally induced exciton redistribution in momentum space. Not all excitons can couple with the radiation field to give out photons because of momentum conservation. Theoretically, only those excitons at $k=0$ can recombine radiatively. In reality, not only $k=0$ excitons contribute to the radiative recombination, as reflected by the fact that the homogeneous exciton linewidth at finite temperature has a certain spectral width ΔE . Actually, excitons with kinetic energy smaller than ΔE , the spectral linewidth of the transition, could recombine radiatively. The fraction r of free excitons with kinetic energy smaller than ΔE is given by⁸

$$r(T) = \frac{\int_0^{\Delta E} D(E)f(E)dE}{\int_0^{\infty} D(E)f(E)dE}, \quad (2)$$

where E is the exciton kinetic energy, $f(E)$ is the Bose-Einstein distribution function, and $D(E)$ is the density of states (DOS). The temperature dependent radiative lifetime is then

$$\tau(T) = \tau_0/r(T), \quad (3)$$

where τ_0 is the radiative lifetime at $T=0$. With increasing temperature, the free excitons will have an increased average kinetic energy; the ratio of excitons with kinetic energy smaller than ΔE will decrease. Therefore the exciton radiative lifetime will increase with temperature. Different DOSs will give out different temperature dependences.

It is interesting to note that the FWHM or the linewidth of the PL spectra of our ZnO nanorods also increases with temperature as T^2 , same as the exciton radiative lifetime. Figure 4(a) plots the FWHM of the PL spectra as a function of temperature from 4.3 to 60 K. In the temperature range of

consideration, the linewidth of the PL spectra is expected to vary like $\Delta E(T) = \alpha + \beta T$ due to acoustic-phonon scattering.²⁴ However, the linewidth of our sample increases with temperature as $\alpha + \beta T^2$, much faster than the expected linear increase. The nanorods have much higher surface to volume ratio, therefore, surface or impurity scattering might be much stronger than in bulk materials. The same temperature dependence of exciton radiative lifetime and linewidth implies a relationship between them. Actually, Feldmann *et al.*⁸ have demonstrated the fundamental relationship between the spectral linewidth and the exciton radiative lifetime in GaAs quantum wells. Similar relationship was observed for our sample. This relationship is manifested when we plot the exciton radiative lifetime as a function of the linewidth of the PL spectra. As shown in Fig. 4(b), the exciton radiative lifetime increases linearly with the spectral linewidth. The physics behind is that the $k=0$ oscillator strength is shared equally among all the states within the spectral linewidth ΔE .⁸ That means the exciton radiative recombination rate is not solely determined by the exciton oscillator strength but depends on the coherence extension of an exciton, which decreases with temperature due to scattering by phonons, defects, or impurities.

In summary, we have studied the exciton radiative lifetime in ZnO nanorods fabricated by vapor phase transport method. It has been found that the exciton radiative lifetime increases with temperature and has a linear dependence on the linewidth of the PL spectra. The physics behind the phenomena has been discussed.

¹Y. F. Chen, D. M. Bagnall, H. Koh, K. Park, K. Hiraga, Z. Zhu, and T. Yao, *J. Appl. Phys.* **84**, 3912 (1998).

²W. Y. Liang and A. D. Yoffe, *Phys. Rev. Lett.* **20**, 59 (1968).

³D. C. Reynolds, D. C. Look, B. Jogai, C. W. Litton, G. Cantwell, and W. C. Harsch, *Phys. Rev. B* **60**, 2340 (1999).

⁴D. M. Bagnall, Y. F. Chen, Z. Zhu, T. Yao, M. Y. Shen, and T. Goto, *Appl. Phys. Lett.* **73**, 1038 (1998).

⁵Z. L. Wang, *J. Phys.: Condens. Matter* **16**, R829 (2004).

⁶S. Deboer and D. A. Wiersma, *Chem. Phys. Lett.* **165**, 45 (1990).

⁷Y. R. Kim, M. Lee, J. R. G. Thorne, R. M. Hochstrasser, and J. M. Ziegler, *Chem. Phys. Lett.* **145**, 75 (1988).

⁸J. Feldmann, G. Peter, E. O. Gobel, P. Dawson, K. Moore, C. Foxon, and R. J. Elliot, *Phys. Rev. Lett.* **59**, 2337 (1987).

⁹T. Itoh, M. Furumiya, T. Ikehara, and C. Gourdon, *Solid State Commun.* **73**, 271 (1990).

¹⁰K. Misawa, H. Yao, T. Hayashi, and T. Kobayashi, *J. Chem. Phys.* **94**, 4131 (1991).

¹¹L. Guo, S. Yang, C. Yang, P. Yu, J. Wang, W. Ge, and G. K. L. Wong, *Appl. Phys. Lett.* **76**, 2901 (2000).

¹²B. Gil and A. V. Kavokin, *Appl. Phys. Lett.* **81**, 748 (2002).

¹³V. A. Fonoberov and A. A. Balandin, *Appl. Phys. Lett.* **86**, 226101 (2005).

¹⁴V. A. Fonoberov and A. A. Balandin, *Appl. Phys. Lett.* **85**, 5971 (2004).

¹⁵V. A. Fonoberov and A. A. Balandin, *Appl. Phys. Lett.* **70**, 195410 (2004).

¹⁶X. H. Zhang, S. J. Chua, A. M. Yong, S. Y. Chow, H. Y. Yang, S. P. Lau, and S. F. Yu, *Appl. Phys. Lett.* **88**, 221903 (2006).

¹⁷Y. P. Varshni, *Physica (Amsterdam)* **34**, 149 (1967).

¹⁸L. Wang and N. C. Giles, *J. Appl. Phys.* **94**, 973 (2003).

¹⁹V. A. Fonoberov, K. A. Alim, A. A. Balandin, F. Xiu, and J. Liu, *Phys. Rev. B* **73**, 165317 (2006).

²⁰D. C. Reynolds, D. C. Look, B. Jogai, and T. C. Collins, *Appl. Phys. Lett.* **79**, 3794 (2001).

²¹R. Eccleston, B. F. Feuerbacher, J. Kuhl, W. W. Rühle, and K. Ploog, *Phys. Rev. B* **45**, 11403 (1992).

²²H. Akiyama, S. Koshiba, T. Someya, K. Wada, H. Noge, Y. Nakamura, T. Inoshita, A. Shimizu, and H. Sakaki, *Phys. Rev. Lett.* **72**, 924 (1994).

²³G. W. 't Hoof, W. A. J. A. van der Poel, L. W. Molenkamp, and C. T. Foxon, *Phys. Rev. B* **35**, 8281 (1987).

²⁴S. Rudin, T. L. Reinecke, and B. Segall, *Phys. Rev. B* **42**, 11218 (1990).